



# Performance Analysis of Ion-Sensitive Field Effect Transistor with Various Oxide Materials for Biomedical Applications

M. Durga Prakash<sup>1</sup> · Beulah Grace Nelam<sup>1</sup> · Shaik Ahmadsaidulu<sup>1</sup> · Alluri Navaneetha<sup>2</sup> · Asisa Kumar Panigrahy<sup>3</sup>

Received: 30 August 2021 / Accepted: 20 September 2021 / Published online: 2 October 2021  
© Springer Nature B.V. 2021

## Abstract

Ion Sensitive Field Effect Transistors (ISFET) are most widely used in medical applications due to simple integration process, measurement of sensitivity and its dual properties. These ISFETs are originated from Metal Oxide Semiconductor Field Effect Transistors (MOSFET) with improvements in structure. ISFETs are used as bio-sensors for the detection of biomarkers in blood, DNA replication and several other medical applications. In this article, we design the ISFET pH sensor in two dimensions with integration of two models namely, semiconductor model and electrolyte model are represented using manageable global equations. The sensitivity of ISFET with different oxide layers is measured and compared. We also measure the sensitivity of the designed 2D-ISFET in two different solutions and compare it with different oxides to know the best oxide material to be used to design the device.

**Keywords** Ion Sensitive Field Effect Transistor (ISFET) · Oxides · Sensitivity · pH sensor · Bio-sensors

## 1 Introduction

The origin of Ion Sensitive Field Effect Transistor (ISFET) has been emerged from the structure of Metal Oxide Semiconductor Field Effect Transistor (MOSFET) having additional improvements making these devices to be widely used in medical field as biosensors [1, 2] ([http://www.idc-online.com/technical\\_references/pdfs/mechanical\\_engineering/ISFET-Bergveld.pdf](http://www.idc-online.com/technical_references/pdfs/mechanical_engineering/ISFET-Bergveld.pdf)). In the initial stages, experiments are done on the structure of MOSFET, and the characteristics can be studied from and improvements are made for ISFET [3, 4]. The drawbacks of the conventional FET such as less sensitivity, delayed response time and high leakage currents make ISFETs popular in the field of sensor designing. The main difference between the structure of

Conventional FET or a MOSFET and Ion Sensitive Field Effect Transistor (ISFET) is the position of gate. We know that any of the transistor structure consists of Source, Drain and Gate on the surface of the substrate. In the same manner, the conventional FET structure consists of Gate deposited on the surface of substrate along with source and drain. But when we observe the gate is separated from the surface of the substrate. The gate separated from the structure of the substrate as the “Reference electrode”. The gate voltage is applied along the reference electrode. Association between the gate dielectric and the ions is regulated by varying the gate voltage which results in determining the ion concentration.

The process of surface interactions takes place from “Site-Binding model”, hydroxyl ions are present on the surface of metal oxide that interacts with the insulator material. In this article, four different oxides namely Silicon Dioxide ( $\text{SiO}_2$ ), Aluminium Oxide ( $\text{Al}_2\text{O}_3$ ), Tantalum Oxide ( $\text{Ta}_2\text{O}_5$ ) and Hafnium Oxide ( $\text{HfO}_2$ ) are deposited on the surface of the substrate with two different electrolyte solutions filled in the electrolyte tank are implemented. In the existing literature, the temperature characteristics and the improvement in the sensing of pH parameter are obtained, where the values of temperature and pH are limited [5]. The sensitivity of ISFET through the process of chemical surface modification can be studied through and the function of ISFET to measure the buffer capacity is surveyed in [6–8]. The primary application of ISFET

✉ M. Durga Prakash  
mdprakash82@gmail.com

<sup>1</sup> Department of ECE, Velagapudi Ramakrishna Siddhartha Engineering College, Kanuru 520007, Andhra Pradesh, India

<sup>2</sup> Department of ECE, Mahatma Gandhi Institute of Technology, 500075 Hyderabad, Telangana, India

<sup>3</sup> Department of ECE, Gokaraju Rangaraju Institute of Engineering & Technology, Hyderabad, Telangana 500090, India

is in the field of medical applications where, recent surveys have implemented their study on DNA with ISFET-based sensing through thermal and chemical based sensing for DNA diagnosis [9, 10]. The sensitivities for these oxides are compared from appropriate plots. The article shows the structure of ISFET and the implementation of oxides onto the ISFET substrate followed by results and discussion that includes the I-V characteristics of the designed structure along with the comparison curve for different oxides. The process of simulation is done in COMSOL Multiphysics Software Tool. Design of the device is done in 2D instead of 3D because the concentration levels in the terminals and the selection of domains of the semiconductor can be easily differentiated and analysed from the front view rather than top view, which can be modelled using 2D.

## 2 Design and Modelling of 2D-ISFET

The design of Two-Dimensional Ion Sensitive Field Effect Transistor (2D-ISFET) can be done in with certain specifications. The gate voltage is applied at the reference electrode. In the phase of designing the device, the electrolyte is placed on the surface of oxide. Drain voltage of 10mV is applied with source connected to the ground. Initially, we fill the electrolyte tank with water and measure the sensitivity. We can observe the surface electric potential of the structure with constant drain voltage and varied pH of bulk electrolyte (pH<sub>b</sub>). The doping concentrations at the source and drain regions are proportional to the variation in pH<sub>b</sub> because when there is a variation in pH<sub>b</sub>, there is variation in the doping concentration. In our experiment, fixed dimensions are used to design the sensor because, the ISFET dimensions are influenced by the sensing region (in our case, gate region) and capacitive effects. When there are smaller capacitive effects, the parameters to the dimensions become less sensitive.

The design of two-dimensional ISFET (<http://www.comsol.co.in/model/simulation-of-an-ion-sensitive-field-effect-transistor-isfet-45341>) in COMSOL Multiphysics software is shown in Fig. 1. The width and height of the substrate is 3 and 0.7 μm. The length of source and drain is 0.5 μm each. The electrolyte tank can be designed in any desired shape. Here, we designed the shape of trapezoid. The centerline of the electrolyte determines the Stern layer having voltage drop [11]. The width and height of the designed electrolyte is 2.8 and 1.4 μm. Bulk electrolyte potential is the variable for the adjustment of gate voltage for fixed drain current. Activity of hydrogen ions (H<sup>+</sup>) and the surface charge density are the variables on the surface of oxide are initialized with simple expressions. The electrolyte domain is selected separately in order to specify the relative permittivity of the solution present in the electrolyte tank manually according to the requirements. In our design, water

is the electrolyte solution used. So, we initialize the value of relative permittivity to 1. Now, we specify the doping at source and drain. The source doping is done with the background doping concentration choosing acceptor concentration of the semiconductor. The drain doping is done in the same manner. The equation for the uniform doping of source and drain is:

$$N_A = N_A^{\text{prev}} + N_{A0} \quad (1)$$

$$N_D = N_D^{\text{prev}} \quad (2)$$

$N_A$  is for the acceptor concentration and  $N_D$  is for the donor concentration. The above equation is for the drain doping.

The source doping involves n-type and p-type with acceptor concentration ( $N_a^-$ ) and donor concentrations ( $N_d^+$ ). The equation for the source doping is considered from Eq. (3) to (5):

$$V = V_{\text{eq}} + V_0 \quad (3)$$

$$n = \frac{1}{2} (N_d^+ + N_a^-) + \frac{1}{2} \sqrt{(N_d^+ - N_a^-)^2 + 4\gamma_n \gamma_p n_{i,\text{eff}}^2} \quad (4)$$

$$p = -\frac{1}{2} (N_d^+ - N_a^-) + \frac{1}{2} \sqrt{(N_d^+ - N_a^-)^2 + 4\gamma_n \gamma_p n_{i,\text{eff}}^2} \quad (5)$$

The doping at the doping region involves several parameters like the base position ( $r_0$ ), the background doping concentration ( $N_b$ ) and the junction depth at different length scales for different directions say X and Y ( $d_j$ )

$$N_A = N_A^{\text{prev}} \quad (6)$$

$$N_D = N_D^{\text{prev}} + N_{D0} \left( - \left[ \left( \frac{r_x^-}{I_x} \right)^2 + \left( \frac{r_x^+}{I_x} \right)^2 + \left( \frac{r_y^-}{I_y} \right)^2 + \left( \frac{r_y^+}{I_y} \right)^2 \right] \right) \quad (7)$$

$$I_x = \frac{d_{jx}}{\sqrt{\ln \left| \left( \frac{N_{A0}}{N_b} \right) \right|}} \quad (8)$$

$$I_y = \frac{d_{jy}}{\sqrt{\ln \left| \left( \frac{N_{A0}}{N_b} \right) \right|}} \quad (9)$$

The trap-assisted recombination involves Shockley-Read-Hall model with electron lifetime ( $\tau_n$ ) and hole lifetime ( $\tau_p$ ) along with the energy difference between the defect level and the intrinsic level ( $\Delta E_t$ ). The equation for the trap-assisted recombination is:

$$n_1 = \gamma_n n_{i,\text{eff}} \exp \left( \frac{\Delta E_t}{k_B T} \right) \quad (10)$$

$$p_1 = \gamma_p n_{i,\text{eff}} \exp \left( - \frac{\Delta E_t}{k_B T} \right) \quad (11)$$

$$n_{i,\text{eff}} = \sqrt{N_{c0}N_{v0}} \exp\left(-\frac{E_g - \Delta E_g}{2k_B T}\right) \quad (12)$$

$$R_n = \frac{np - \gamma_n \gamma_p n_{i,\text{eff}}^2}{\tau_p(n + n_1) + \tau_n(p + p_1)} = R_p \quad (13)$$

$$\nabla \cdot J_n = qR_n \quad (14)$$

$$\nabla \cdot J_p = -qR_p \quad (15)$$

The top boundaries of substrate are specified as thin insulator gate with oxide relative permittivity,  $\epsilon_{\text{ins}}=4.5$ , Oxide Thickness,  $d_{\text{ins}}=30\text{nm}$  and the metal work function,  $\Phi=0\text{ V}$ .

The semiconductor has:

Relative permittivity  $\epsilon_r$

Band Gap ( $E_g, 0$ )

Electron Affinity  $\chi_0$

Effective density of states at valence and conduction band  $N_v$  and  $N_c$

$$\rho = q(p - n + N_d^+ - N_a^-) \quad (16)$$

$$\nabla \cdot J_n = 0 \quad (17)$$

$$\nabla \cdot J_p = 0 \quad (18)$$

$$J_n = qn\mu_n \nabla E_c + \mu_n k_B T G\left(\frac{n}{N_c}\right) \nabla_n + qnD_{n,\text{th}} \nabla \ln(T) \quad (19)$$

$$J_p = qp\mu_p \nabla E_v - \mu_p k_B T G\left(\frac{p}{N_v}\right) \nabla_p - qpD_{p,\text{th}} \nabla \ln(T) \quad (20)$$

$$E_c = -(V + \chi_0) - \alpha \Delta E_g \quad (21)$$

$$E_v = -(V + \chi_0 + E_{g,0}) + (1 - \alpha) \Delta E_g \quad (22)$$

The relative permittivity is another term for dielectric constant, which indicates the polarization effect of a material when imposed to an electric field on the surface of an insulator. In the experiment, the oxides  $\text{SiO}_2$ ,  $\text{HfO}_2$ ,  $\text{Al}_2\text{O}_3$  and  $\text{Ta}_2\text{O}_3$  are used. The relative permittivity of these oxides is individual, each indicating the effect of polarization on the surface of the gate insulator, when an electric field is applied. The relative permittivity is calculated using Eq. 23 for any material.

$$\epsilon_r = \frac{\epsilon}{\epsilon_0} \quad (23)$$

Where,

$\epsilon_r$  = relative permittivity

$\epsilon$  = permittivity of the substance or oxide material

$\epsilon_0$  = Relative permittivity of free space

For the design of two-dimensional ISFET shown in the Fig. 1, different design parameters are taken into consideration where they play a crucial role to obtain the electron and hole concentration of the designed model. The surface chemical reactions that take place at the Helmholtz layer in the Helmholtz plane occur depending on the values of diffusion coefficients for  $\text{H}^+$  and  $\text{OH}^-$  ions. These are listed in the Table 1. For the device modelling, the body of the semiconductor is  $0.7\text{ }\mu\text{m}$  height and its width is  $3\text{ }\mu\text{m}$ . The source and drain are  $0.5\text{ }\mu\text{m}$  in length towards the gate. The gate region is  $1.3\text{ }\mu\text{m}$  wide and is large enough to act as a reacting surface to the electrolyte solution.

The surface electric potential of the design shown in previous section is simulated. From the plots obtained in Fig. 2, as we observe, the doping concentration of drain is clearly varied

**Fig. 1** Design and modelling of two-dimensional Ion Sensitive Field Effect Transistor (2D-ISFET)

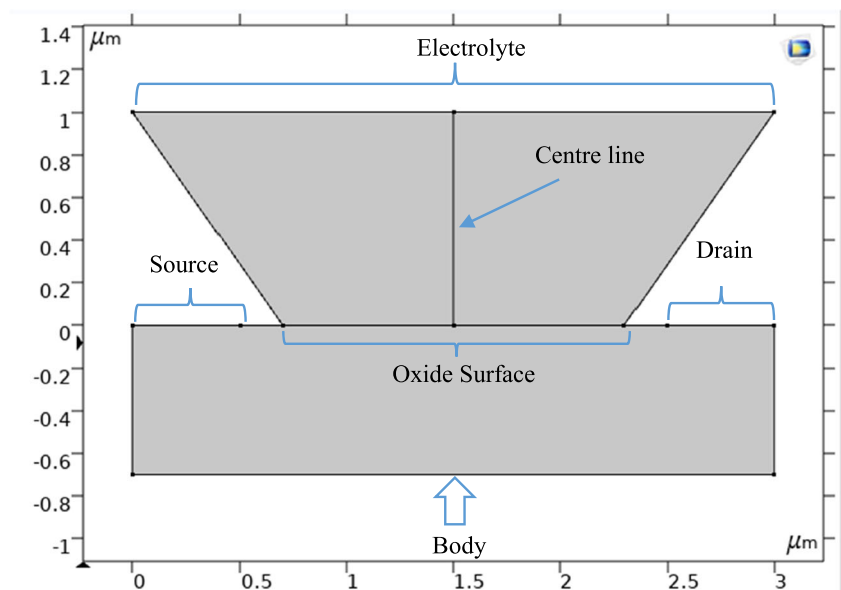


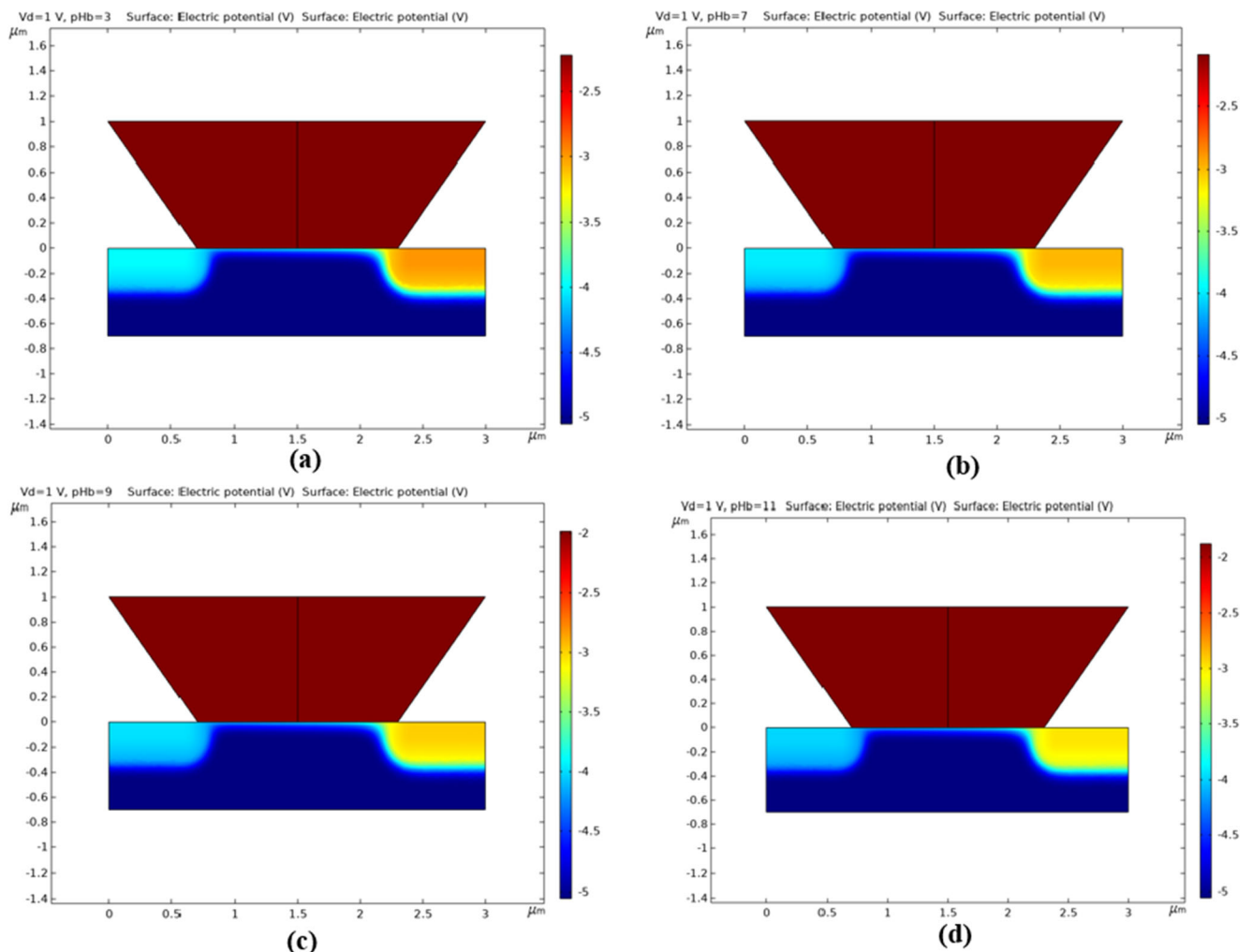
**Table 1** Design Parameters for modelling two-dimensional ISFET

| Parameter   | Value   |
|---|---|
| Drain Voltage( $V_d$ )                                  | 10[mV]  |
| Temperature( $T_0$ )                                    | 25[degC]                                      |
| Bulk $H^+$ concentration( $cH\_bulk$ )                  | 100[mol/m <sup>3</sup> ]                      |
| Bulk $OH^-$ concentration ( $cOH\_bulk$ )               | 1E-8[mol/m <sup>3</sup> ]                     |
| pH of bulk electrolyte(pH <sub>b</sub> )                | 3, 7, 11                                      |
| Relative permittivity of water( $\epsilon_{s\_H2O}$ )   | 78.5  |
| Relative permittivity of blood( $\epsilon_{s\_blood}$ ) | 60.5  |
| Diffusion coefficient of $H^+$ ( $DH$ )                 | 36.3e-4[cm <sup>2</sup> /V <sub>therm</sub> ] |
| Diffusion coefficient of $OH^-$ ( $DOH$ )               | 20.5e-4[cm <sup>2</sup> /V <sub>therm</sub> ] |
| Thermal Voltage( $V_{therm}$ )                          | 0.025693[V]                                   |
| Oxide surface binding site density ( $N_s$ )            | 5e18[1/m <sup>2</sup> ]                       |

with change in bulk electrolyte potential (pH<sub>b</sub>). From Fig. 2(a) to (d), there is an increase in the doping concentration with an increase in bulk electrolyte potential. The important parameter

to be considered is the dielectric material, in our experiment, the oxide materials act as dielectric materials where, they are non-polar molecules that do not cause any physical change with a change in geometric composition. And, these metal oxides have wide range of properties, using these in the field of biosensor is essential for the experiment.

The following diagrams represent the designed model in 2D plot for different oxides taken into consideration. From the plots, we observe that for different oxides, the doping concentration varies at the source and drain regions. If we have a keen observation from the plots, all the oxide layers at the source side have same level of doping concentration but on the drain side, they vary with slight changes, with one oxide having rough doping concentration and the other having the heavily doping concentration. This is because, the source is grounded, and the drain has come input voltage to be given in order for the device to function. Let us see in Fig. 3, the 2D plots for water as electrolyte solution. There is variation in the doping concentration near the source and drain regions with different oxide materials along with the variation of concentration of

**Fig. 2** Surface electric potential of 2D-ISFET with  $V_d=1$  and pH = 3, 7, 9 and 11

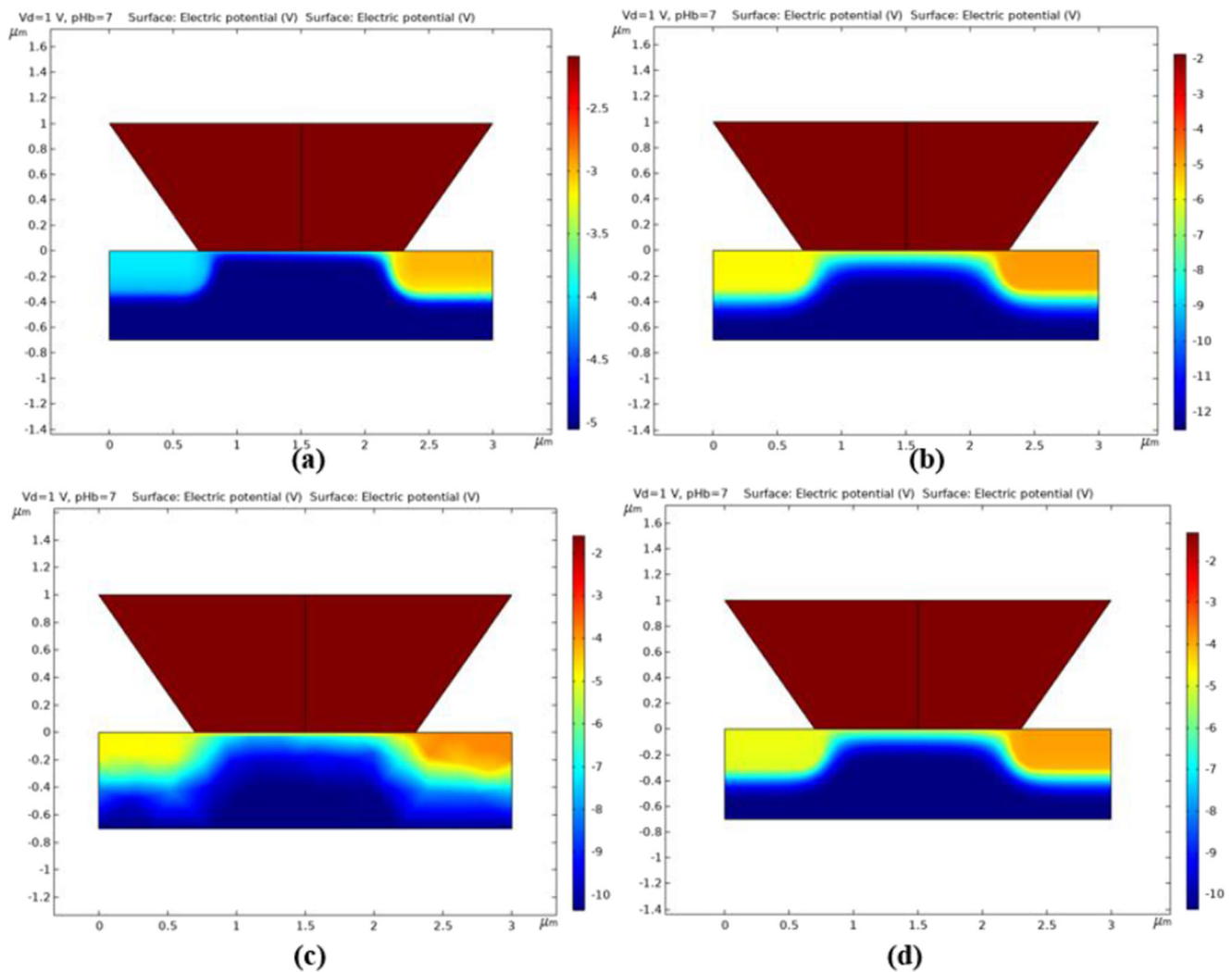


**Fig. 3** 2D plot of 2D-ISFET for different oxide materials (a)  $\text{SiO}_2$  (b)  $\text{HfO}_2$  (c)  $\text{Al}_2\text{O}_3$  (d)  $\text{Ta}_2\text{O}_2$

the barrier between the source and drain terminals. The 2D plots of the designed structure are same when the electrolyte solution is taken with water or blood. This is because the doping concentration parameter is not changed when the electrolyte solution is taken as water or as blood.

There is change in the color of concentration for oxides, when  $\text{Al}_2\text{O}_3$  oxide is considered, we observe disturbed concentration levels throughout the design structure. When oxides  $\text{Ta}_2\text{O}_3$  and  $\text{HfO}_2$  are taken into consideration, we observe clear variation of concentration levels at each terminal. When  $\text{SiO}_2$  is taken into consideration, the concentration level at the source side are quite low when compared to all other oxide (represented in light blue color) and the drain terminal has light orange color concentration, which is low level of concentration when compared to the concentration levels of other oxides' drain terminals. In our experiment, the pH of bulk electrolyte,  $\text{pH}_b=7$  for all the oxides considered. When the oxide is  $\text{SiO}_2$ , at the drain terminal has pale orange or bright yellow color representing a concentration between  $-3$  and  $-$

3.5. But when we compare the concentration value of  $\text{SiO}_2$  with  $\text{HfO}_2$ , we observe the concentration at the drain terminal is bright orange, indicating the level of concentration to be  $-5$ , for oxide  $\text{Al}_2\text{O}_3$  the concentration level is at a value of  $-4$  and for  $\text{Ta}_2\text{O}_3$  oxide, the concentration value is between  $-3$  and  $-4$ . Though the oxides when compared to  $\text{SiO}_2$  indicates a decrease in concentration value, the color scale indicates a higher concentration at the drain terminal compared to  $\text{SiO}_2$ . The same is the case at the source terminal of the design. The concentration value of  $\text{SiO}_2$  is very less compared to all the other oxides considered. This can be clearly observed from the color scale.

### 3 Results and Discussion

After the computation of the structure designed, there are various plots obtained that gives the comparison of some of the parameters to be observed when doped with different oxide



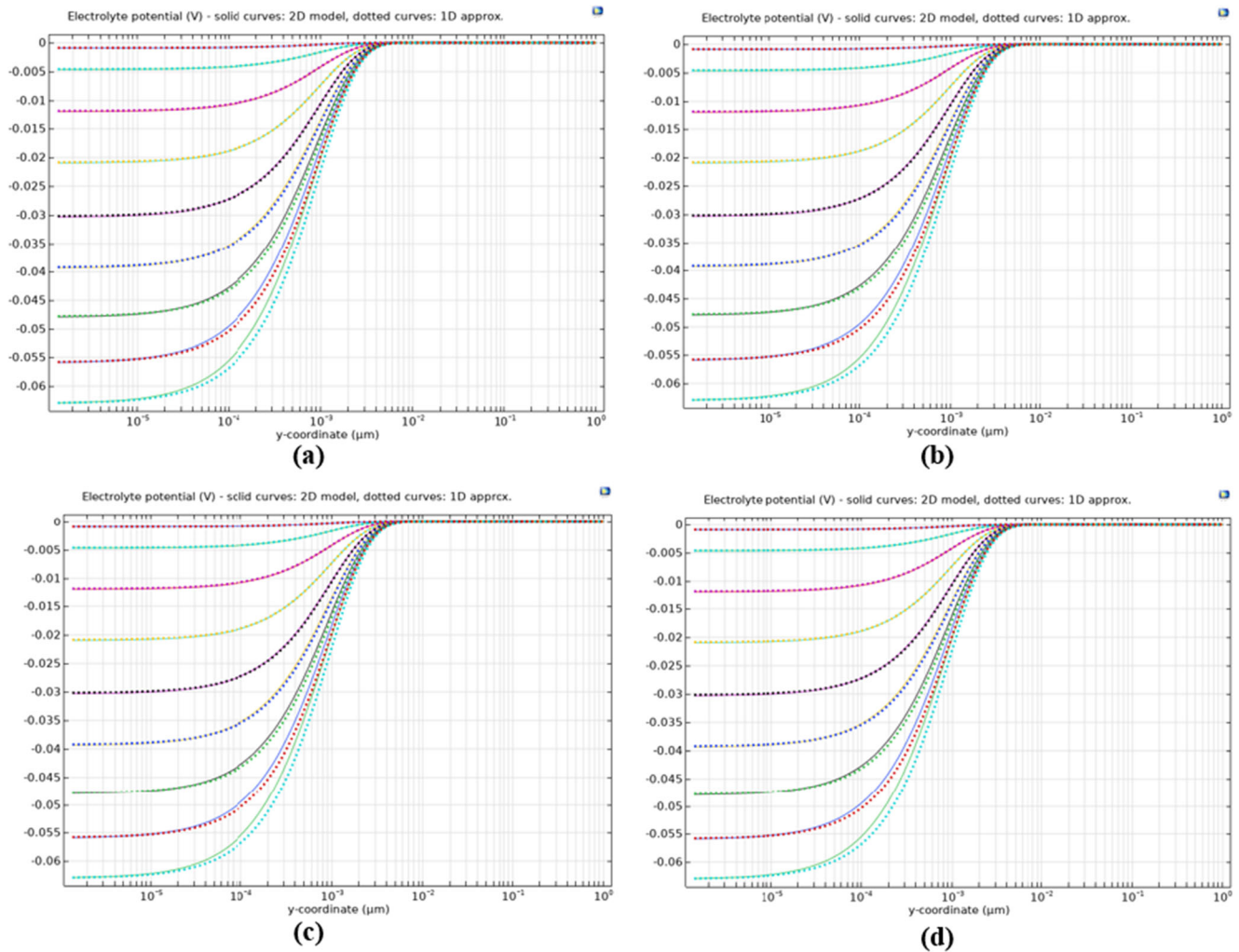


**Fig. 4** Electric potential at the centerline of electrolyte for different oxides with water as electrolyte solution. (a)  $\text{SiO}_2$  (b)  $\text{HfO}_2$  (c)  $\text{Al}_2\text{O}_3$  (d)  $\text{Ta}_2\text{O}_5$

layers. For the designed model shown in the previous sections, we obtain electrolyte potential with respect to two electrolyte solutions namely, water and blood along with the  $I_d$  vs.  $V_d$  characteristics of the designed Two-Dimensional Ion Sensitive Field Effect Transistor (2D-ISFET).

### 3.1 Electrolyte Potential

The electrolyte potential along the center line of the electrolyte represents a zero-charge region. This electrolyte potential determines the voltage drop near the Stern layer. The following plots represent the electrolyte potential for different oxides considered when electrolyte solution is water and blood.

The electrolyte potential curves change with varied oxide layers. This is done for variables adjusting the gate voltage for a specified drain current, the bulk electrolyte potential is taken as a variable in the experiment to obtain drain current for fixed gate voltage. This electrolyte potential is obtained by the difference between the boundary Ordinary Differential Equation

(ODE) for oxide surface (phil) and the bulk electrolyte potential (phil\_bulk). The properties of the bulk electric potential (phil\_bulk) variable is applied at the surface edges of the electrolyte. The solid curves in the plot represent the 2D model and the dotted curves represent the 1D model. These two models are compared at the electrolyte central line where there is voltage drop i.e., at the Stern Layer. We observe that the 2D model and 1D model are aligned on the same varied potential axis. But there is change in 1D model and 2D model for  $\text{SiO}_2$  oxide layer as shown in Figs. 4 and 5.

### 3.2 Drain Current ( $I_d$ ) vs. Gate Voltage ( $V_g$ )

The gate voltage is applied across the front gate of the ISFET design model. The drain current is the functional parameter for the appropriate gate voltage. In the structure designed, the gate voltage is applied across the oxide surface and the conductor is the electrolyte. The following plots represent the  $I_d$  vs.  $V_g$

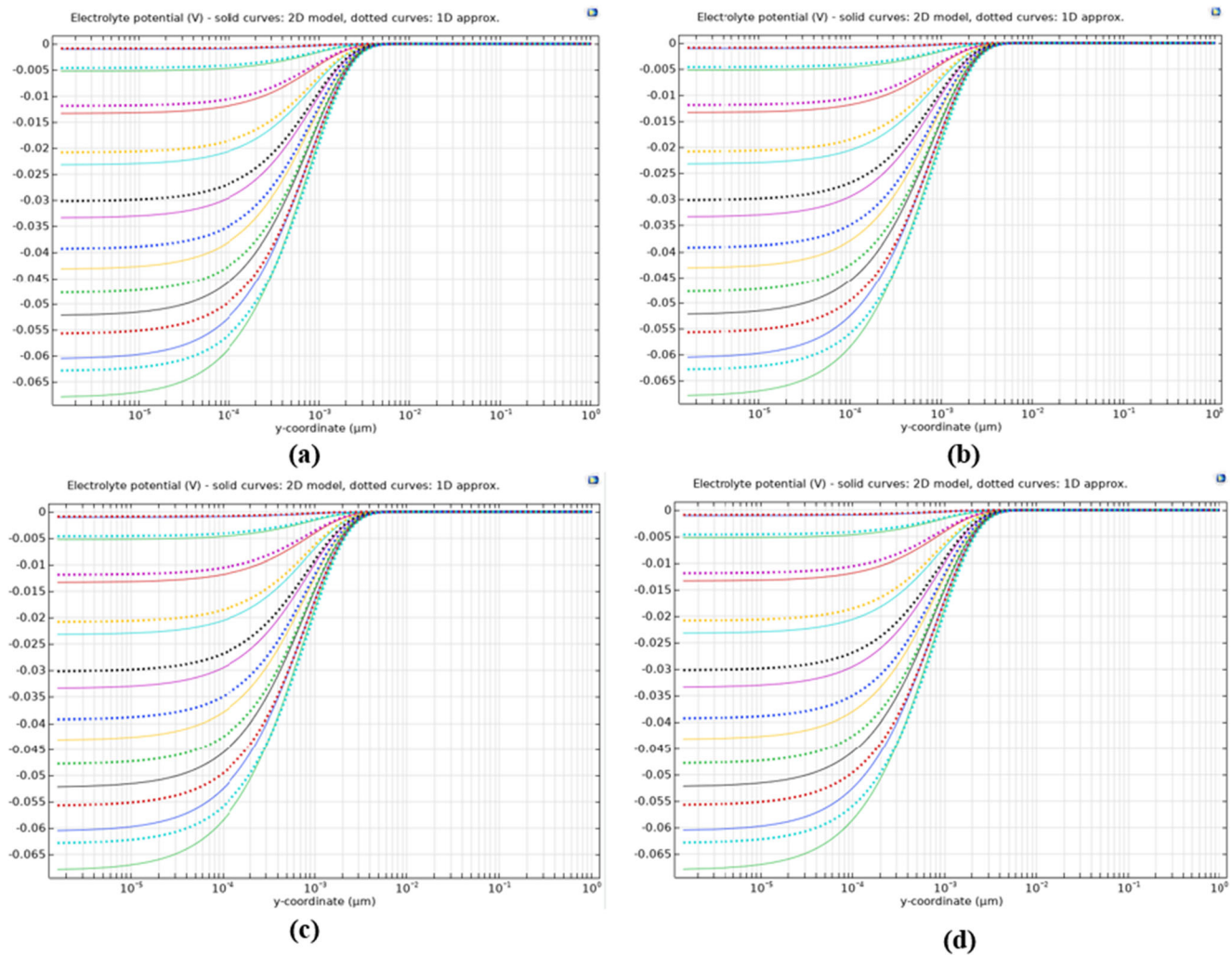


**Fig. 5** Electrolyte potential at the centerline of electrolyte for different oxides with blood as electrolyte solution. (a)  $\text{SiO}_2$  (b)  $\text{HfO}_2$  (c)  $\text{Al}_2\text{O}_3$  (d)  $\text{Ta}_2\text{O}_3$ .

characteristics for different oxides when water and blood are taken as electrolyte solutions.

From Fig. 6, we observe that there is a drastic change in the drain current for different oxides. In Fig. 6(a) we observe that there is huge drain current for  $\text{Ta}_2\text{O}_3$  when compared with other oxides and  $\text{Al}_2\text{O}_3$  oxide has not much current, taking into consideration the electrolyte solution is water. In Fig. 6(b), we observe that there is great increase in drain current for the specified voltage at  $\text{SiO}_2$  oxide when compared with other oxides, when blood is taken as electrolyte solution.

### 3.3 $I_d$ vs. $V_d$ with Varied pH Values

We take three pH values 3, 7 and 11. And we compute the design considering the parameter that controls the device is the pH value. In Fig. 7, we see  $I_d$  vs.  $V_d$  curve for different oxide layers with water as the electrolyte solution.

From the Fig. 7, we observe that there is a huge variation in the drain current for different pH values at certain voltage. When we consider  $\text{Al}_2\text{O}_3$  as the oxide surface, for the pH =

11, there is barely any current. For oxide surface  $\text{Ta}_2\text{O}_3$ , there is decrease in drain current for an increase in pH value. For oxide surface as  $\text{HfO}_2$ , there is certain drain current at pH values 3 and 7 but  $I_d = 0$  for pH = 11. For  $\text{SiO}_2$  oxide surface, for increased pH value, the drain current decreases but the current does not drop to zero. Also, the plot for certain oxides with respect to pH values overlap with each other. We can say that different oxides at the same pH values can have same current flow with fixed gate voltage. We can also observe that  $\text{SiO}_2$  at pH = 3 and  $\text{Ta}_2\text{O}_3$  at pH = 3 has greater current flow but compared to  $\text{SiO}_2$ ,  $\text{Ta}_2\text{O}_3$  has greater current flow with less difference. From the above plots, we can conclude that the pH value is inversely proportional to drain current. When the plots are combined in an imaginable case, the plots for oxides  $\text{HfO}_2$  and  $\text{Al}_2\text{O}_3$  for pH = 11 overlap with each other having the same drain voltage.

The following plots in Fig. 8 represents the  $I_d$  vs.  $V_d$  characteristics with blood as electrolyte solution for different oxides taking into consideration. From the plots of  $I_d$  vs.  $V_d$  characteristics at different pH values, we observe that when

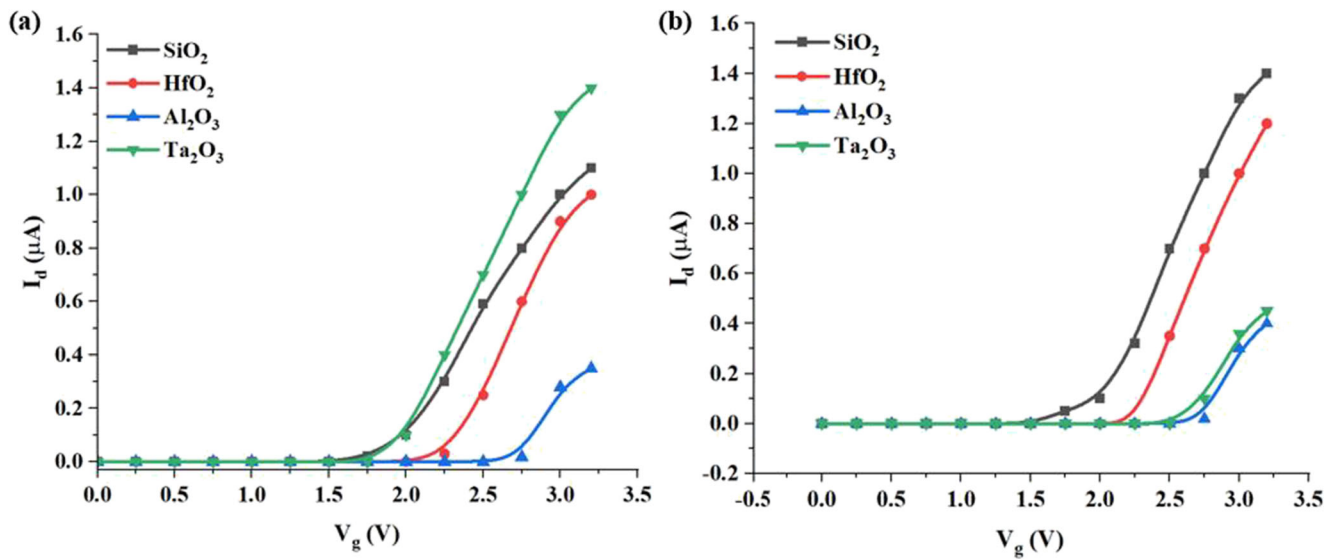


Fig. 6  $I_d$  vs.  $V_g$  characteristics for different electrolyte solutions (a) Water (b) Blood

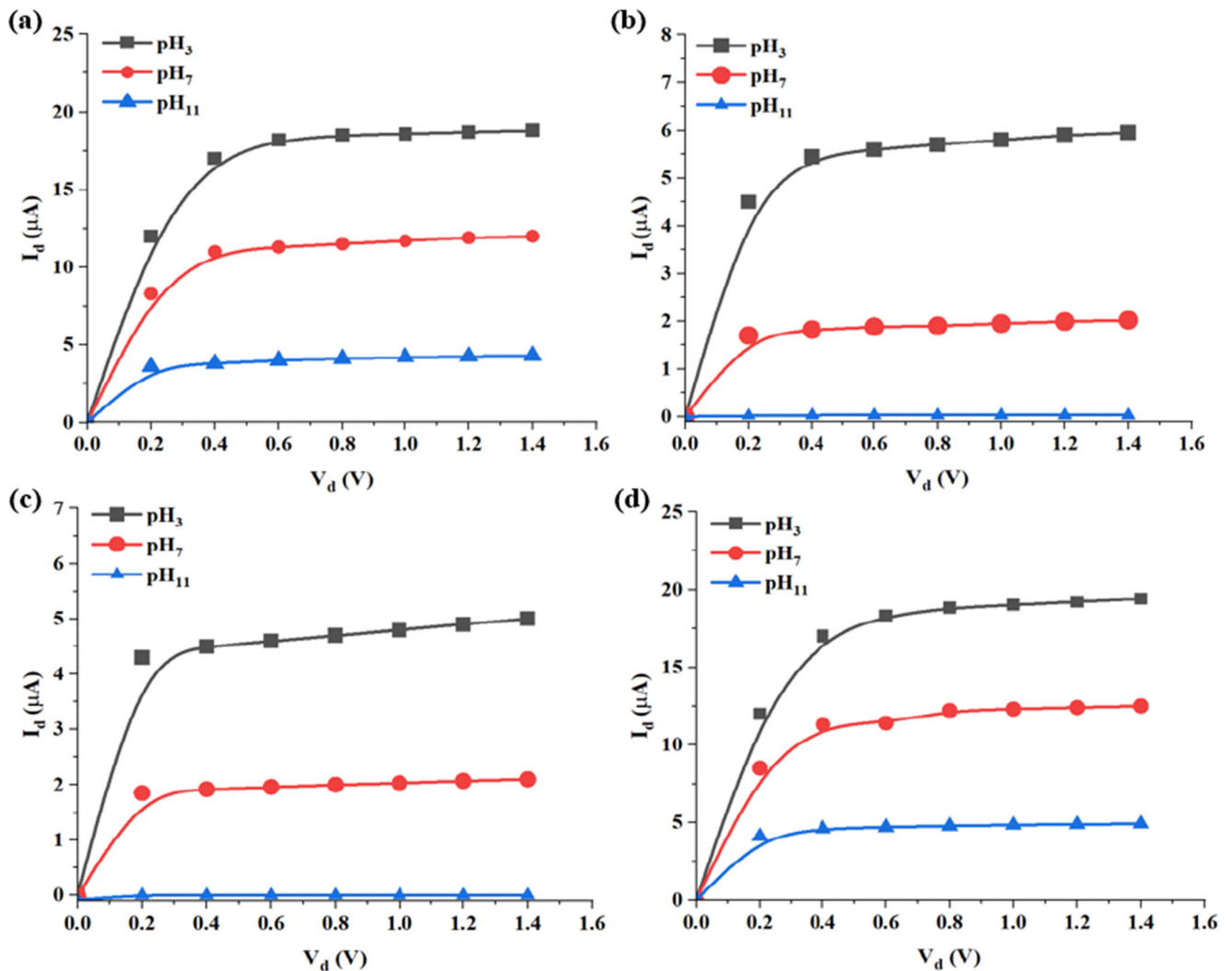


Fig. 7  $I_d$  vs.  $V_d$  with varied at different oxides with water as electrolyte solution (a)  $\text{SiO}_2$  (b)  $\text{HfO}_2$  (c)  $\text{Al}_2\text{O}_3$  (d)  $\text{Ta}_2\text{O}_3$



blood is used as electrolyte solution at  $\text{pH} = 11$  for  $\text{Al}_2\text{O}_3$  and  $\text{Ta}_2\text{O}_3$  oxides there is barely any current. For the oxides  $\text{HfO}_2$  and  $\text{SiO}_2$ , the drain current flows with decreased  $\text{pH}$  value.  $\text{SiO}_2$  at  $\text{pH} = 3$  and  $\text{pH} = 7$  draws great amount of current compared to all other oxides. But when all the plots are combined in an imaginable case, the plots of oxides  $\text{Al}_2\text{O}_3$  and  $\text{Ta}_2\text{O}_3$  for  $\text{pH} = 11$ , the plots can be overlapped and same is the case with  $\text{pH} = 7$ . For oxides  $\text{SiO}_2$  and  $\text{HfO}_2$ , for  $\text{pH} = 3$ , the plots overlap at certain points.

If we consider the value of  $\text{pH} = 3$ , some of the values for various oxide show similar characteristics or similar curve for  $I_d$  vs.  $V_d$  characteristics obtained in the Fig. 8. But when we observe the value of drain current for different oxides and the points plotted on the graph, we observe variation in the scale of drain current where the scale is varied from 0 to 23 ( $\mu\text{A}$ ) for  $\text{SiO}_2$ , 0 to 6.5 ( $\mu\text{A}$ ) for  $\text{HfO}_2$ , 0 to 20 ( $\mu\text{A}$ ) for  $\text{Al}_2\text{O}_3$  and 0 to 13 ( $\mu\text{A}$ ) for  $\text{Ta}_2\text{O}_3$ . Even though the curve is similar, the drain current values change with respect to oxide. And among the oxides  $\text{Ta}_2\text{O}_3$  shows high sensitivity characteristics which can be clearly observed in the next section.

### 3.4 Sensitivity of the 2D-ISFET

The sensitivity of the modelled 2D-ISFET varies with varying the oxide surface. In our experiment, we have introduced four different oxide layers  $\text{Al}_2\text{O}_3$ ,  $\text{Ta}_2\text{O}_3$ ,  $\text{HfO}_2$  and  $\text{SiO}_2$ . It is the most important parameter to be taken into consideration for the functionality of ISFET in the application of medical sciences as a bio-sensor. We computed the designed model taking into account two different electrolyte solutions, water and blood. Figure 9 represents the sensitivity of the device for different oxide surfaces with two different electrolyte solutions considering the sensitivity of the oxides in the increasing order, which is represented in a tabular format.

In the above plots in Fig. 9(a) the sensitivity is more when the oxide  $\text{Ta}_2\text{O}_3$  is considered when compared to other oxide layers when the electrolyte solution is water. Same is the case when the electrolyte solution is blood, we clearly observe (Fig. 9(b)) that the sensitivity of the device is more when  $\text{Ta}_2\text{O}_3$  is considered as the oxide surface.

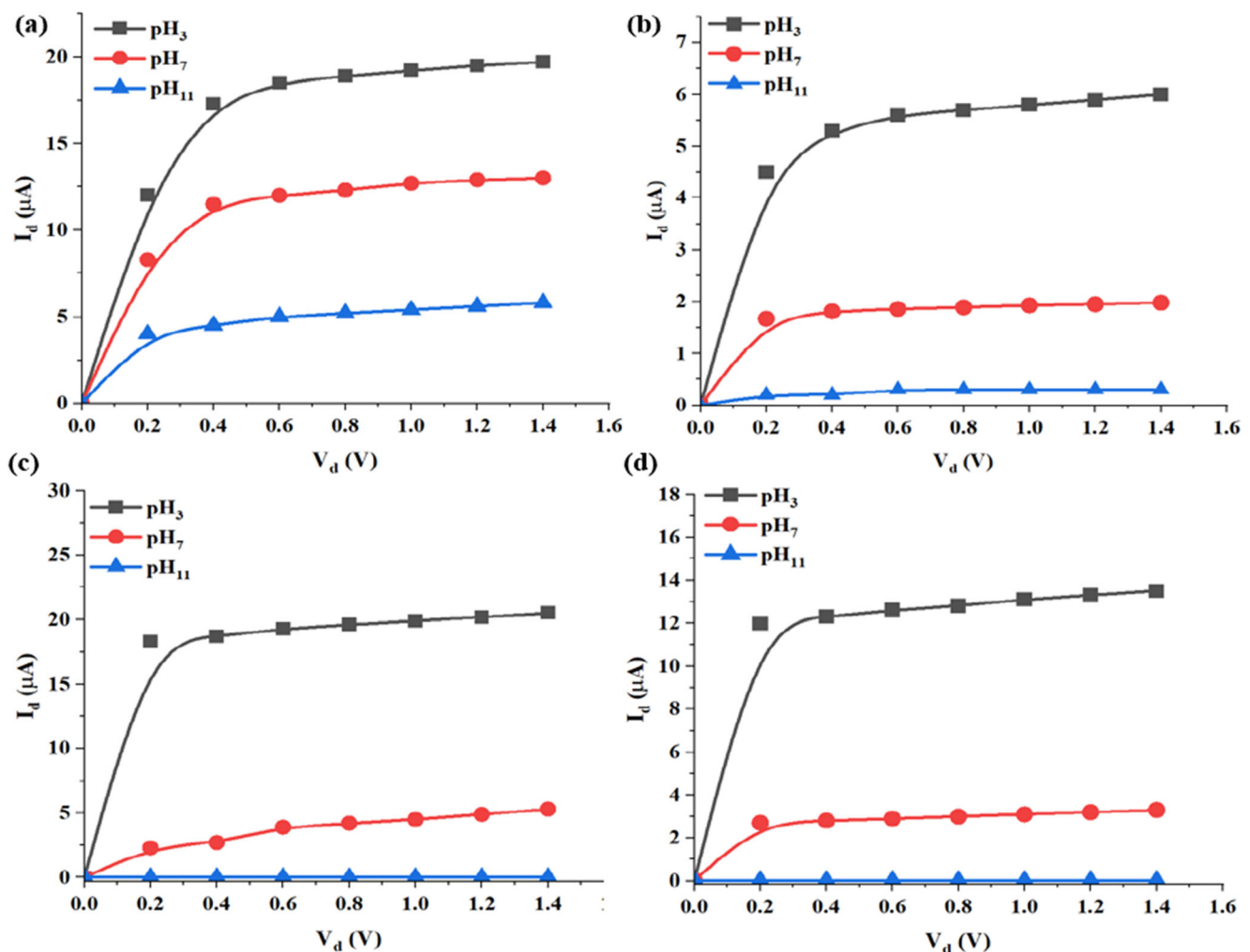
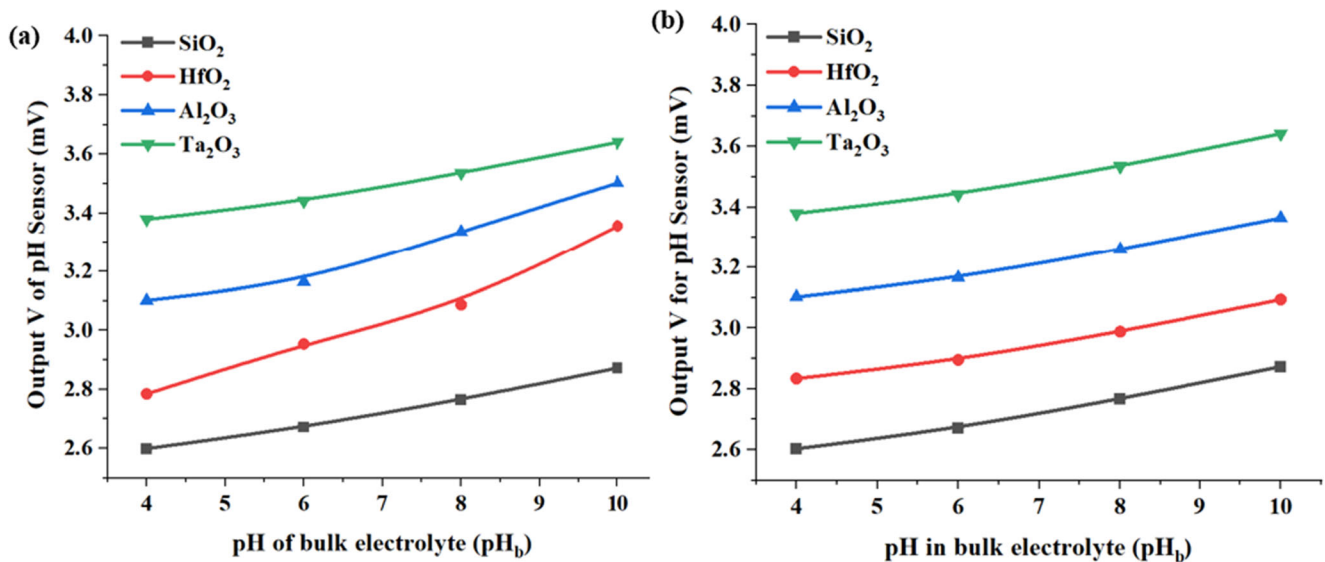


Fig. 8  $I_d$  vs.  $V_d$  with varied  $\text{pH}$  at different oxides with blood as electrolyte solution (a)  $\text{SiO}_2$  (b)  $\text{HfO}_2$  (c)  $\text{Al}_2\text{O}_3$  (d)  $\text{Ta}_2\text{O}_3$



**Fig. 9** Sensitivity curve for different oxide layers at different electrolyte solutions (a) Water (b) Blood

The sensitivity parameter for the designed model when different oxides are taken into consideration and also when there is a change in the electrolyte solution. We compare the sensitivity obtained from four different oxides and conclude which oxide material is best to take into account to obtain the highest sensitivity, shown in Table 2 where different electrolyte solutions are used for analysis.

The sensitivity of the device is more when the oxide surface is Ta<sub>2</sub>O<sub>3</sub> for both electrolyte solutions, water and blood. So, we can design the future modelling of Ion Sensitive Field Effect Transistors (ISFET) with Ta<sub>2</sub>O<sub>3</sub> as the oxide surface for better sensitivity of the device.

## 4 Conclusions

In this work, design of a Two-Dimensional Ion Sensitive Field Effect Transistor (2D-ISFET) has been performed. The concentration variation along with  $I_d$  vs.  $V_g$  characteristics with different oxides is studied with two electrolyte solutions, water and blood. How the modelled device can be used as a pH sensor or a bio-sensor in the field of medical applications can be observed from the variation of pH for different oxides is

**Table 2** Sensitivity for varied oxide surfaces and electrolyte solutions

| Oxide material                 | Sensitivity for electrolyte solution (mV/pH) |       |
|--------------------------------|--|-------|
|                                | Water  | Blood |
| SiO <sub>2</sub>               | 37   | 40    |
| HfO <sub>2</sub>               | 40   | 43    |
| Al <sub>2</sub> O <sub>3</sub> | 44   | 45    |
| Ta <sub>2</sub> O <sub>3</sub> | 50   | 52    |

observed. The sensitivity of the device with various oxides is experimented and the Tantalum Oxide (Ta<sub>2</sub>O<sub>3</sub>) is used as the oxide surface with highest sensitivity among the various oxide materials taken into consideration for both electrolyte solutions. For further improvement of the device specifications, the oxide having higher sensitivity can be used in designing the ISFET as an application with reduced dimensions varying from micro-meters to nano-meters.

**Acknowledgements** The authors would like to acknowledge Indian Institute of Technology Hyderabad (IIT Hyderabad) for backing us with some experimental work carried out and the tool (COMSOL Semiconductor Module) required for simulating this work. And M. Durga Prakash thankfully acknowledges this publication as an outcome of the R&D work undertaken project under the Start-up Research Grant (File No.: SRG/2019/002236) Scheme of Department of Science and Technology (DST), Government of India, being Science Engineering Research Broad (SERB).

**Author Contributions** M. Durga Prakash, Alluri Navaneetha, Asisa Kumar Panigrahy, and Beulah Grace Nelam: Conceptualization; M. Durga Prakash, Beulah Grace Nelam and Shaik Ahmadsaidulu: investigation; M. Durga Prakash, Beulah Grace Nelam, Alluri Navaneetha and Shaik Ahmadsaidulu: resources; M. Durga Prakash and Beulah Grace Nelam: data curation; Beulah Grace Nelam, Alluri Navaneetha, and Asisa Kumar Panigrahy: writing—original draft preparation; M. Durga Prakash, and Asisa Kumar Panigrahy: writing—review and editing; M. Durga Prakash and Shaik Ahmadsaidulu: visualization; M. Durga Prakash: supervision;

**Data Availability** No supplementary materials.

**Declarations** This article does not contain any studies with human or animal subjects.

**Conflict of Interest** The authors declare that they have no conflict of interest.

**Consent to Participate** Additional informed consent was obtained from M. Durga Prakash identifying information is included in this article.

## References

1. Bergveld P (2003) Thirty years of ISFETOLOGY. *Sens Actuators B Chem* 88(1):1–20. [https://doi.org/10.1016/s0925-4005\(02\)00301-5](https://doi.org/10.1016/s0925-4005(02)00301-5)
2. Kaisti M (2017) Detection principles of biological and chemical FET sensors. *Biosens Bioelectron* 98:437–448. <https://doi.org/10.1016/j.bios.2017.07.010>
3. Gill A, Madhu C, Kaur P (2015) Investigation of short channel effects in Bulk MOSFET and SOI FinFET at 20nm node technology. 2015 Annual IEEE India Conference (INDICON). <https://doi.org/10.1109/indicon.2015.7443263>
4. Indukuri T, Koonath P, Jalali B (2006) Monolithic vertical integration of metal-oxide-semiconductor transistor with subterranean photonics in silicon. 2006 Optical Fiber Communication Conference and the National Fiber Optic Engineers Conference. <https://doi.org/10.1109/ofc.2006.215480>
5. Sinha S, Bhardwaj R, Sahu N, Ahuja H, Sharma R, Mukhiya R (2020) Temperature and temporal drift compensation for Al<sub>2</sub>O<sub>3</sub>-gate ISFET-based pH sensor using machine learning techniques. *Microelectron J* :104710. <https://doi.org/10.1016/j.mejo.2020.104710>
6. Van den Berg A, Bergveld P, Reinhoudt DN, Sudhölter EJ (1985) Sensitivity control of ISFETs by chemical surface modification. *Sens Actuators* 8(2):129–148. [https://doi.org/10.1016/0250-6874\(85\)87010-4](https://doi.org/10.1016/0250-6874(85)87010-4)
7. Van Hal REG, Eijkel JCT, Bergveld P (1995) A novel description of ISFET sensitivity with the buffer capacity and double-layer capacitance as key parameters. *Sens Actuators B Chem* 24(1–3):201–205. [https://doi.org/10.1016/0925-4005\(95\)85043-0](https://doi.org/10.1016/0925-4005(95)85043-0)
8. Luo J, Olthuis W, Bergveld P, Bos M, van der Linden WE (1994) Determination of buffer capacity by means of an ISFET-based coulometric sensor-actuator system with a gate-covering porous actuator. *Sens Actuators B Chem* 20(1):7–15. [https://doi.org/10.1016/0925-4005\(93\)01170-9](https://doi.org/10.1016/0925-4005(93)01170-9)
9. Keeble L, Moser N, Rodriguez-Manzano J, Rodriguez-Manzano J, Georgiou P (2020) ISFET-based sensing and electric field actuation of DNA for on-chip detection: a review. *IEEE Sens J* :1–1. <https://doi.org/10.1109/jsen.2020.2998168>
10. Cacho-Soblechero M, Malpartida-Cardenas K, Cicatiello C, Rodriguez-Manzano J, Georgiou P (2020) A dual-sensing thermo-chemical ISFET array for DNA-based diagnostics. *IEEE Trans Biomed Circuits Syst* :1–1. <https://doi.org/10.1109/tbcas.2020.2978000>
11. Oldham KB (2008) A Gouy–Chapman–Stern model of the double layer at a (metal)/(ionic liquid) interface. *J Electroanal Chem* 613(2):131–138. <https://doi.org/10.1016/j.jelechem.2007.10.017>

**Publisher's Note** Springer Nature remains neutral with regard to jurisdictional claims in published maps and institutional affiliations.